Master's Thesis of Landscape Architecture

Mapping time-series land use land cover map and analysis forest change trend in inaccessible North Korea

접근불가지역인 북한의 시계열 토지피복도 매핑 및 산림 변화 동향 분석

August 2021

Graduate School of Seoul National University
Department of Landscape Architecture and Rural systems Engineering, Landscape Architecture Major

Yong Piao

Mapping time-series land use land cover map and analysis forest change trend in inaccessible North Korea

Under the Direction of Adviser, Prof. Dong Kun Lee

Submitting a master's thesis of Landscape Architecture

July 2021

Graduate School of Seoul National University
Department of Landscape Architecture and Rural systems Engineering, Landscape Architecture Major

Yong Piao

Confirming the master's thesis written by
Yong Piao
July 2021

Chair _____
Vice Chair _____
Examiner _____

Abstract

North Korea, as an inaccessible area, has little research on land cover change, but it is very important to understand the changing trend of LULCC and provide information previously unknown to North Korea. This study therefore aimed to construct and analyze a 30-m resolution modern time-series land use land cover (LULC) map to identify the LULCCs over long time periods across North Korea and understand the forest change trends. A land use and land cover (LULC) map of North Korea from 2001 to 2018 was constructed herein using semi-permanent point classification and machine learning techniques on satellite image time-series data. The resultant relationship between cropland and forest cover, and the LULC changes were examined. The classification results show the effectiveness of the methods used in classifying the time series of Landsat images for LULC, wherein the overall accuracy of the LULC classification results was 97.5% ± 0.9%, and the Kappa coefficient was 0.94 ± 0.02. Using LULC change detection, our research effectively explains the change trajectory of North Korea's current LULC, providing new insights into the change characteristics of North Korea's croplands and forests. Further, our results show that North Korea's urban area has increased

significantly, its forest cover has increased slightly, and its cropland cover has decreased. We determined that North Korea's Forest protection policies have led to the forest restoration. Thus, as agriculture is one of North Korea's main economic contributors, croplands have been forced to relocate, expanding to other regions to compensate for the land loss caused by forest restoration.

Keyword : Land use and land cover change, Remote sensing, Forest, Agriculture, North Korea, NDVI

Student Number : 2019-21805

Table of Contents

Chapter 1. Introduction

Forests cover approximately one-third of the Earth's land area but account for about two-thirds of the Earth's total photosynthesis; they have a very large exchange with the atmosphere and are sensitive to climate change and human activities [1]. Forests provide vital organic infrastructure for the planet such as climate control, disaster prevention, and carbon balance. Human activities, such as deforestation, land use, land-use change, and forestry, affect changes in carbon stocks between the carbon pools of the terrestrial ecosystem and the atmosphere [2]. The detection of changes in the magnitude of LULC by deforestation can help solve the current greenhouse gas emissions problem. Further, protecting and restoring forests could play a crucial role in the solution [3, 4].

Land use and land cover (LULC) is one of the important studies that can analyze the trend of forest change. LULC data, which are closely related to social and human activities, provide important information for environmental assessments [64]. Variation detections based on LULC data allows researchers to better understand the relationship between nature and humans in a specific area [58, 60, 63, 65, 66] . Several studies have shown that, globally,

approximately 60% of land changes are related to direct human activities, while the remaining 40% are related to indirect driving forces, such as climate factors [63]. In the Asian region, more than 50% of the land is covered by cropland, and the deforestation rate is high [67]. Therefore, reducing the negative environmental impact of land–use changes while maintaining economic viability and social acceptability is the main challenge faced by most developing countries in Asia [67].

North Korea (the Democratic People's Republic of Korea (DPRK) is known to have some of the most degraded forests in the world, converted to croplands from mountainous areas, approximately 80% of North Korea's terrain [5]. It is the mountainous cropland which is the one of characteristic in North Korea cropland. Many researchers have studied LULC to identify deforestation in North Korea [6–9]. However, large uncertainties arise from variations among the types of land use change processes, stemming from a lack of consistent measurements of land change processes at regional scales spanning sufficiently long time periods.

Remote sensing combining classification algorithms and indices obtained from multitemporal data makes it possible to reduce uncertainties associated with LULC changes in inaccessible areas. Previous studies have been widely applied to LULC, including a

variety of data, indices, and algorithms of classification in deforestation regions [10–12]. There is still insufficient information to identify LULC change reflected forest phenology of growing season during long time–periods because it is difficult to collect cloud–free data at a macro level during rainy season and apply suitable indices and algorithms [13]. In particular, collecting data from long time series at a macro scale for LULC in large–scale area has some limitations because of the extensive resource requirement such as manpower, time, and big data processing.

To address these challenges, the Google Earth Engine (GEE) platform can be used by combining time–series satellite images and geospatial datasets [14]. These also provide many cloud–free data for long periods of time and improve the accuracy of LULC by combining phenological information using various environmental variables, such as the normalized difference vegetation index (NDVI), normalized difference water index (NDWI), and digital elevation models (DEM) [7, 15].

Traditional classification algorithms are parametric classifiers that assume a normal distribution for training data such as ISODATA and K–Means, which have problems of over–fitting, highly collinear, sensitivity to outliers, high dimensionality, and noise compared to machine learning (MLEA) and ensemble

algorithms [16, 17]. The advantage of MLEA is non-parametric based on non-linear data , such as random forest based on machine learning, support vector machines(SVM), K-nearest neighbor (KNN), artificial neural network (ANN), and classification and regression tree (CART), which have the ability to improve classification accuracy by reducing the collinear and noise processing of time-series data without overfitting. In particular, RF combined with phenological information could improve the classification of farmland and semi-arid vegetation by capturing the specific seasonal patterns of each landscape type compared to other MLEAs [18, 7, 19, 20].

In existing North Korean studies, owing to the characteristics of the region, there is a limitation that on-site investigations cannot be performed [7, 21, 22]. Jin et al. [7] used a MODIS dataset and Random Forest machine learning technology to classify the LULC data for North Korea by utilizing the China side of the North Korea and China border to obtain field survey points to verify their findings. Jeong et al. [5] used a MODIS dataset, as well as normalized difference vegetation index (NDVI), normalized difference snow Index (NDSI), and normalized difference water index (NDWI), which are indices, and iterative self-organizing data analysis technique (ISODATA) unsupervised classification method

to classify North Korea's LULC, and the verification sample points and Kappa coefficient obtained by stratified random sampling were used to validate the accuracy of their results. However, these studies are generally limited to a certain year. In the existing North Korean LULC classification research, some studies have used an LULC dataset provided by South Korea's Ministry of Environment (MOE) to analyze the time series of LULC changes [6, 8] to analyze the trend of forest changes in North Korea. Therefore, due to the lack of verification measures such as on-site investigation or documentation, there is some uncertainty in the estimation results, such as correct LULCC patterns or status observations [23]. In this regard, our research method helps to reduce uncertainty and classify and observe the forests of North Korea.

Synthetically, RF and phenological information such as NDVI and NDWI can be used to improve the accuracy of the mapping of specific forest types for LULC using various environmental variables based on the GEE platform and build sample data for LULC across North Korea using existing LULC products and semi-permanent sample point classification methods. Using this method, the long-term time-series LULC classification and verification can help identify LULC pattern changes in inaccessible areas.

The purpose of our research is to examine the LULCC across

North Korea in order to understand the changing pattern of modern North Korea's agriculture and forest, which is of great significance for understanding the changing trend of LULCC and providing previously unknown information. We posed the following key questions for North Korea's LULCC regarding its inaccessible area: (1) How to conduct verifiable and highly accurate LULC data in an inaccessible area? (2) What is the modern changing pattern of North Korea's cropland and forest?

To answer these questions, we (1) used semi-permanent sample point classification methods and machine learning algorithms to classify and verify inaccessible areas, producing North Korean LULC data from 2001 to 2018 at a resolution of 30 m, (2) investigated and collected relevant information regarding North Korea's forests and agriculture from the literature, (3) used change detection methods to analyze the LULCC results, and (4) assessed and analyzed the change patterns of North Korea's modern cropland and forest based on the existing literature.

Chapter 2. Study Area

North Korea is located in the northern part of the Korean peninsula in East Asia, accounting for 55.1% of the total area of the Korean peninsula and covers nine districts and counties. More than 80% of North Korea's land is mountainous and is primarily concentrated in the north (Figure 1). The height of the mountains in the region gradually decreases from north to south, creating plains and croplands in the southern and western regions. North Korea has a temperate monsoon climate, with an average annual temperature of 8 – 12 ℃ and an annual rainfall of 600 – 1000 mm [24]. The rainy season is concentrated in the summer, from July to August, and the dry season occurs in spring, from April to May.

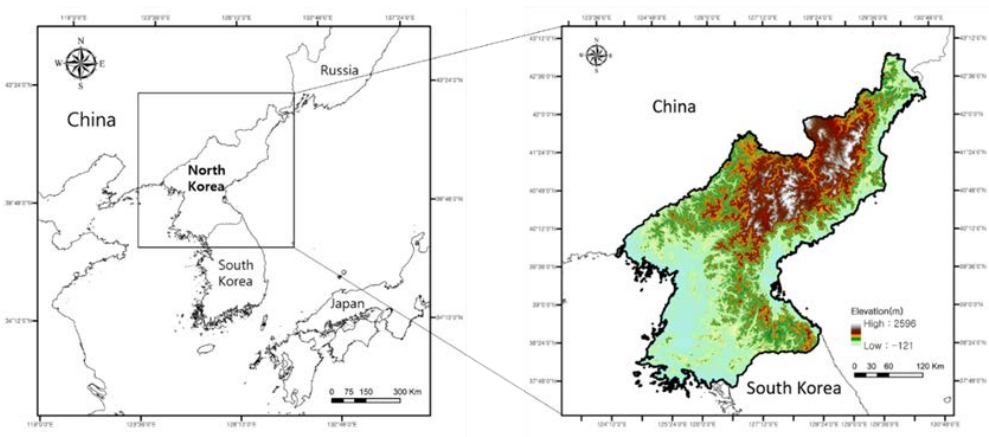

Figure 1 Study area: North Korea, Korean Peninsula. (Democratic People's Republic of Korea; DPRK)

Chapter 3. Materials and Methods

3.1. Study overview

Due to the various limitations of the study region, especially its inaccessibility and lack of geographic information data [43], there are few verified long-term time series land cover maps with high resolution. Although some studies have classified the land cover in North Korea [7, 44], their results are generally limited to a certain year. Therefore, in this study, to obtain a verified long-term time series land cover map, the classification method proposed by hu et al. [28], with the addition of some improvements, was used. This method is based on "complete consistency" and "temporal stability" principles for processing sample points for high-precision long-term land cover classification, even when limited data or on-site surveys are not possible. Based on a LULC map, we assessed and analyzed the change patterns of the study area between 2001 and 2018.

Research flowchart (Figure 2) outlines the research steps of the LULC classification method and change detection. First, Landsat TOA reflectance products are used for land classification based on cloud mosaic, and multi-year image synthesis methods were applied. Second, semi-permanent training sample points and

validation sample points are filtered from five types of 30 m resolution LULC products according to the principles of “complete consistency” and “temporal stability” Third, based on the filtered semi-permanent sample points, random forest machine learning was used to classify the input bands for LULC classification in North Korea. The accuracy of the classification results was validated using training data. Finally, a change detection method was used to assess and analyze LULCC patterns.

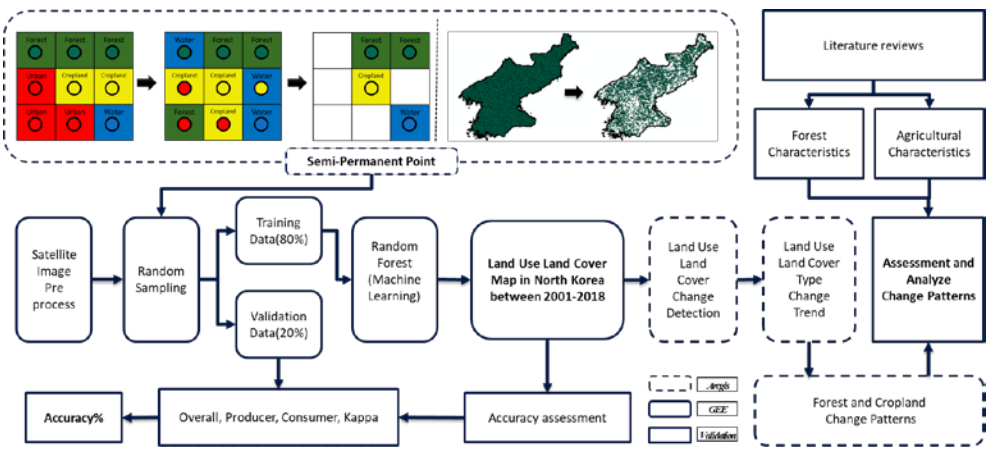

Figure 2 Research Flow Chart

3.2. Data Collection

The method we applied relies on the use of multi-temporal and multi-spectral images for classifying forest areas by combining the land-cover type characteristics identified in the study area. We obtained the Landsat TOA product dataset and the Shuttle Radar

Topography Mission V3 product (SRTM Plus) [25] digital elevation data, Defense Meteorological Program (DMSP), Operational Line-Scan System (OLS) [26], and NPOESS Preparatory Project (NPP) data. We also used visible infrared imaging radiometer suite (VIIRS) [27] data, which provided two different night lighting products (Table 1).

Based on Hu and Hu's [28] classification method, all land cover products had a 30 m resolution, with the exception of the MODIS land cover products. Thus, we used 500 m low resolution MODIS Land Cover Type Product (MCD12Q1) data in combination with 30 m high resolution products such as the Global Forest Change dataset (GFCD) [29], global land cover (GLC30) [30], Finer Resolution Observation and Monitoring of Global Land Cover (FROM-GLC) [31, 32], and Global Food Security-support Analysis Data Extent Southeast and Northeast Asia (GFSAD30SEACE) [33] (Table 1).

Table 1 Classification of Data Sources

Class	Data	Year	Term	Resolution
Satellite Image	Landsat	2000 – 2019	16 days	30 m
	Defense Meteorological Program (DMSP)/Operational Line-Scan System (OLS)	2001 – 2012	1 year	30 arc seconds

	NPOESS Preparatory Project (NPP)/Visible Infrared Imaging Radiometer Suite (VIIRS)	2012 – 2017	1 month	15 arc seconds
	Shuttle Radar Topography Mission V3 product (SRTM3)	2000	-	30 m
Land use and land cover (LULC) Product	MCD12Q1.006	2001 – 2018	1 year	500 m
	Finer Resolution Observation and Monitoring of Global Land Cover (FROM-GLC)	2017	-	30 m
	Global land cover (GLC30)	2010	-	30 m
	Global Forest Change dataset (GFCD)	2000	-	30 m
	Global Food Security-support Analysis Data Extent Southeast and Northeast Asia (GFSAD30SEACE)	2015	-	30 m
Satellite Index	Normalized Difference Vegetation Index (NDVI)	2001 – 2018	-	30 m
	Normalized Difference Water Index (NDWI)	2001 – 2018	-	30 m

3.3. Data Processing

During satellite image pre-processing, we first sorted the image data from April to July of a predetermined year, as well as the year before and after, to identify pixels with cloud coverage

below 40%. Using these selected images, we obtained high-quality no-cloud satellite image data and reclassified the land cover types into the six LULC classification products: built-up, cropland, forest, grassland, bare land, and water bodies. In this study, wetland cover was included in the water body cover based on the research method used and the regional characteristics. These land cover types were used to filter the semi-permanent training and verification sample points. According to the limitations of the classification method used and the characteristics of the study area, water bodies were included in the wetland cover type. Reclassifying the MCD12Q1, GFCD, GLC30, FROM-GLC, and GFSAD30SEACE data into LULC types generated overlay products and filter sample points. From 10,000 randomly selected sample points, we were able to filter 4,853 sample points for classification.

3.4. Classification Process

Successful classification requires the selection of an efficient classifier for classifying spatial properties of spectra and other variables using a small number of training samples [68, 69]. Using machine learning-based classifiers is very useful for finding patterns in complex feature spaces while minimizing data-

dimensional problems [70]. Previous studies have shown that RF performed well in LULC classification [20, 34]. Therefore, in this study, we used the Random Forest [71] machine learning algorithm for LULC classification. The RF It can handle predictors with different characteristics, not sensitive to noise and outliers, and overtraining, fast, and efficient [34, 72, 73]. The classifier generates multiple decision trees, and the generated decision trees are classified into a random subset of training data and input variables. To verify that 80% of the sample points were used for training, 20% were used for validation. The number of decision trees (ntree) was set to 500, which was found to have been sufficient in previous experiments [35]. Furthermore, the NDVI [36], NDWI [37], SRTM products, DMSP/OLS, and NPP/VIIRS products were entered as input data for the random forest classification.

The NDVI was determined as follows:

$$NDVI = \frac{(NIR-Red)}{(NIR+Red)} \quad (1)$$

and the NDWI was determined as follows:

$$NDWI = \frac{(Green-NIR)}{(Green+NIR)} \quad (2)$$

where green, red, and NIR are the surface reflectance of the 3, 4, and 5 bands of the Landsat OLI products, and the surface reflectance of the two, three, and four bands of Landsat TM products, respectively.

In this study, most of these methods applied the Google Earth Engine (GEE) [14], which is a highly efficient free cloud platform for processing and analyzing satellite image data [38].

3.5. LULCC Analysis

For change detection using the classification results to observe the trend of forest changes in North Korea, the LULC classification results of this study were analyzed based on the ArcGIS platform. From these pixel-based classification result images, the total area and change of each LULC class in the study area were calculated. In the change detection, formulas (1) and (2) are used to calculate the total area and change of each LULC class in the study area from these pixel-based classification result images, and formula (3) was used to calculate the rate of change in the study area from 2001 to 2018.

The proportion of each LULC type used was calculated as follows:

$$A_i\% = \frac{A_i}{A_t} \times 100\% \quad (3)$$

The change for each LULC type was calculated as follows:

$$A_i = A_i t1 - A_i t2 \quad (4)$$

The annual rate of change for each LULC type was calculated as follows:

$$A_{ir} = \left(\frac{A_i t1}{A_i t2} - 1\right) X\, 100\% \quad (5)$$

where A_i refers to the area of the LULC type i, A_t denotes the total study area, and A_i% denotes the proportion of each LULC type area. A_i t1 and A_i t2 refer to the total area of LULC type i in specific years 1 and 2, respectively [39]. A_ir refers to the rate of change, which is the magnitude of change between the specified years, and the range of change from 2001 to 2018 was analyzed in this study [40].

3.6. Reference Data Collection and Classification Accuracy Validation

Post-classification accuracy evaluation for LULC is the most important part of LULC classification results, and LULC maps with high accuracy play an important role in successful environmental management and planning [74]. Confusion Matrix is the most widely

applied accuracy evaluation method in existing LULC research [77]. The Confusion Matrix is a very effective method of indicating accuracy in that the accuracy of each category is clearly described, along with the inclusion errors (commission errors) and exclusion errors (missing errors) present in the classification [76]. Therefore, the Confusion Matrix can derive a set of descriptive and analytical statistics for the LULC classification results, which can explain the reliability of the data used in the study [75, 76, 78]. To verify the time-series classification results, a confusion matrix including the over-all accuracy (OA), user's accuracy (UA), producer's accuracy (PA), and kappa coefficient [41] was used. We evaluated the accuracy of classification for a total of five classification types in the level 1 classification system, except for bare land, which could not be classified in this study. The five classification types were built-up, cropland, forest, grassland, and water bodies; wetlands were included in the water bodies category in this study. In addition, visual interpretation was conducted through comparison with other existing LULC classification products, MOD12Q1, FROMGLC2017, and high-resolution satellite images obtained via Google Earth [28]. Global LULC products such as FROMGLC still require further verification at the international level to determine whether they are useful in other applications

[42]. For example, the GlobCover 2009 LULC product with a resolution of 300 m was not included in this study after confirming a visual critical classification error at the study site.

There are few verified long-term time series land cover maps with high resolution on account of the various limitations of the study region, especially North Korea's inaccessibility and lack of geographic information data [43]. Although some studies have classified the land cover in North Korea [44, 7], their results are generally insufficient for a certain year. Therefore, in this study, to obtain a verified long-term time series land cover map, the classification method proposed by Hu and Hu [28], with some improvements, was used. This method is based on "complete consistency" and "temporal stability" principles for processing sample points for high-precision long-term land cover classification, even when limited data is available or when onsite surveys are not possible. Based on an LULC map, we assessed and analyzed the change patterns in the study area between 2001 and 2018.

Chapter 4. Results

4.1. LULC Classification Accuracy Assessment

The classification results in Table 2 show that the classification

accuracy of cropland, forest, and water bodies was higher than that of the other land cover types in North Korea from 2001 to 2018. The overall accuracy and kappa coefficient were _97.5% ± 0.9% and 0.94 ± 0.02, respectively. The accuracy satisfies the standard proposed by researchers in other studies [45, 46, 7]. Both producer s and user s accuracies of all classes were higher than 90%. The results of the classes are presented in Table 2. The built−up area type also had high accuracy, where the user's and producer's accuracies were 91.5% ± 8.3% and 85.9% ± 14.7%, respectively. Meanwhile, the classification accuracy of the grassland was low, with user and producer accuracies of 72. ± 27.1% and 49. ± 15.9%, respectively. Because land cover classification uses semi−permanent sample points that are filtered from a land area that has remained unchanged for many years, the accuracies of the stable classes such as croplands, forests, and water bodies are very high after verification [28].

Table 2 Land Cover Classification Accuracy from 2001 to 2018

Land Cover	User's Accuracy	Producer's Accuracy
built-up	91.7% ± 8.3%	85.3% ± 14.7%
Cropland	93.8% ± 2.8%	97.5% ± 1.9%
Forest	98.9% ± 1.1%	99.7% ± 0.3%
Grassland	72.9% ± 27.1%	49.3% ± 15.9%
Water bodies	96.8% ± 3.2%	95% ± 5%

Overall Accuracy	97.5% ± 0.9%	Kappa Coefficient 0.94 ± 0.02

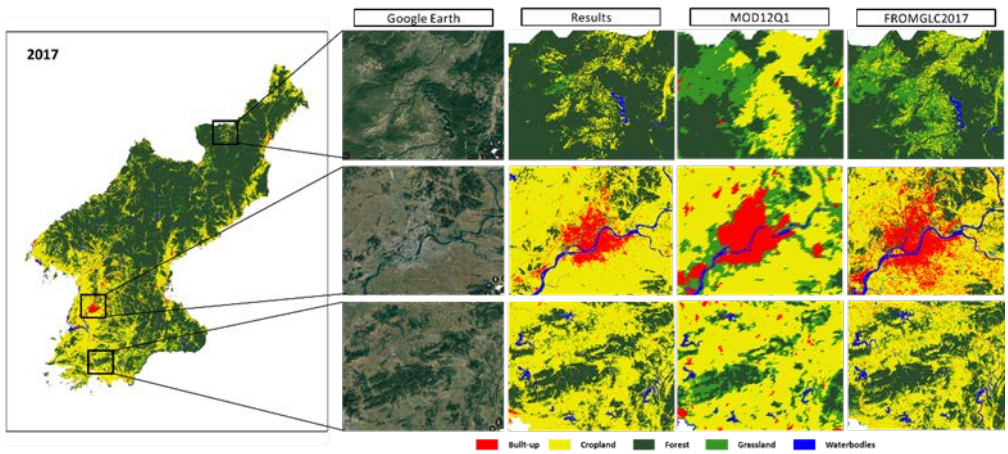

Figure 3 Image validation and comparison of different land cover products in 2017

Our classification results were then visually compared with the MOD12Q1 and FROMGLC land cover classification products, as well as high-resolution images obtained via Google Earth. As shown in Figure 3, compared to Google Earth's high-resolution satellite images, the classification result largely reflects the real land type. Furthermore, the quality of our land cover classification is better than that of the MOD12Q1 product and somewhat similar to that of the FROMGLC product. However, note that our results are better than the FROMGLC products with regard to classification aggregation.

4.2. LULC Classification Results

The 30 m resolution land cover map was classified using semi-permanent sample points and the random forest algorithm with in long term timeseries in 2001-2018, sorting the data into built-up, cropland, forest, grassland, and water bodies (wetland), as shown in Figure 4. Note that bare land is not reflected in the classification results of the study area. The reason is that the bare land and grassland in the study area are similar in spectrum and the bare land area is very small, so the bare land in the LULC product used in this study is so different that the semi-permanent point classification method applied cannot filter out the bare land sample.

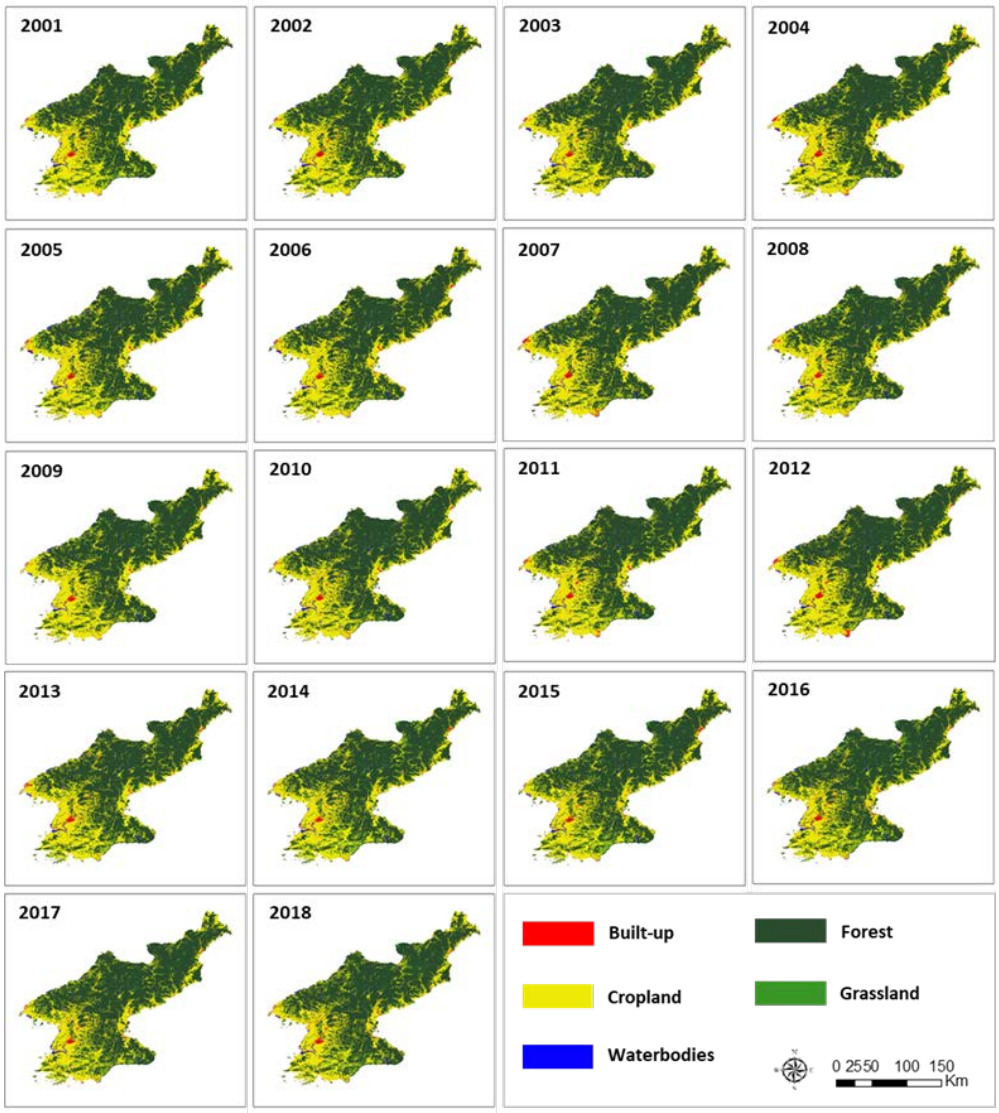

Figure 4 Land use and land cover classification maps for 2001 to 2018

Figure 5 shows that the main land types of LULC in North Korea are forest and cropland. The largest change in the 18-year study period was the restoration of the forest cover type in the south and central mountains. Further, the concentrated expansion of

croplands in the north and west regions were also large changes.

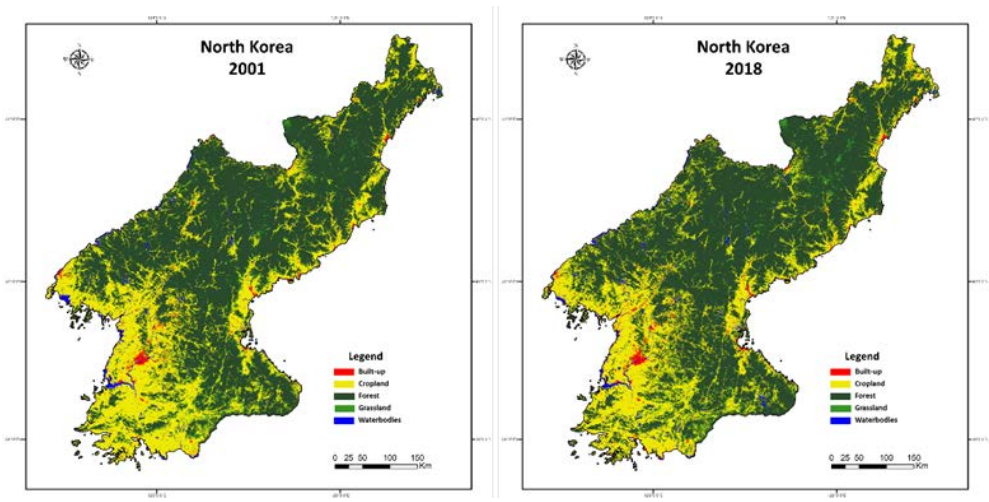

Figure 5 Land use and land cover classification maps for 2001 and 2018

4.3. LULC Change Detection

Figure 6 shows that the year-to-year change trend of the land cover area shows that the forest cover change is relatively stable. Including a decrease in forest area from 2011 to 2015, the total forest area increased compared with that in 2001. The decrease in 2011-2015 can be attributed to deforestation [47], and the overall growth trend can be attributed to the recent launch of forest restoration projects [48]. This result is also consistent with existing research results [49].

The change in cropland cover showed a different trend of an

initial increase and then decrease in cover. After increasing from 2003 to 2013, it began to gradually decrease in 2014. Cropland increased from 2003–2014 due to the reclamation of mountainous cropland, but since 2014, forest restoration seems to have increased due to abandoned farmland [50].

The grassland cover area underwent a fluctuating decrease from 2003 to 2012, and in 2013, the decreasing trend became more stable. The area in 2012 experienced a larger decrease compared with the initial year, while the area change from 2015 to 2016 underwent a larger increase compared with that in the initial year.

The area covered by the water body (and wetland) did not significantly change compared to the initial year. With the exception of an area decrease from 2006 to 2008, the area increased compared to that in 2001.

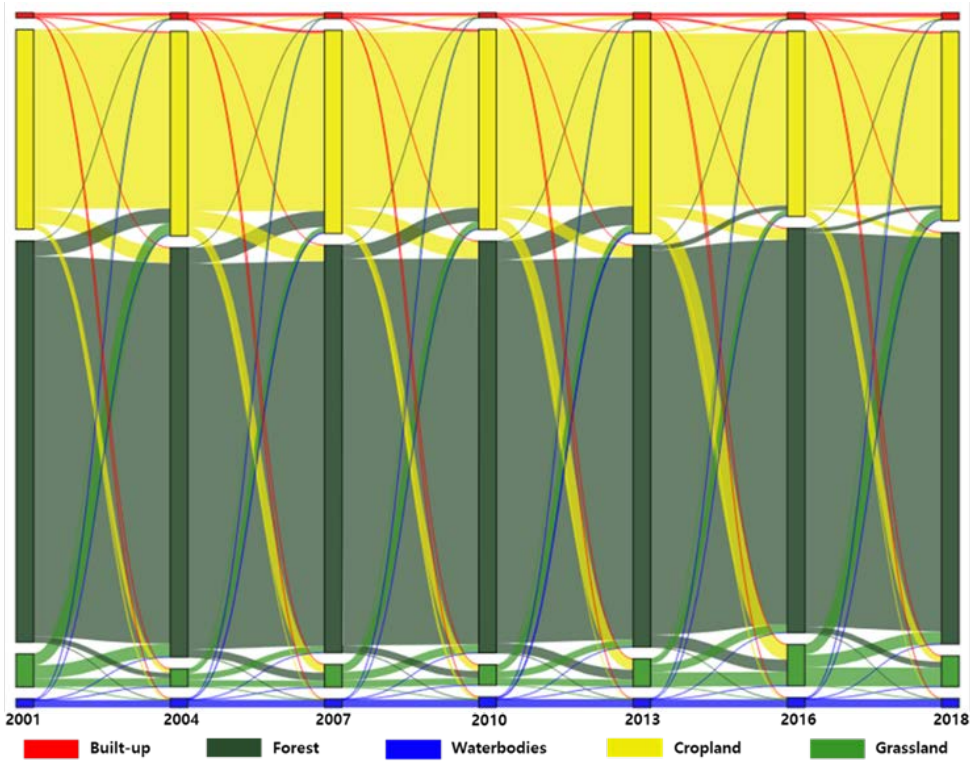

Figure 6 Land use and land cover change plot between 2001 to 2018

The built-up area increased significantly from 2001 to 2018, with a change rate of 37.26 %. In addition, the forest and water body areas increased at rates of 2.59% and 4.73%, respectively. Conversely, the cropland and grassland areas showed decreasing trends at change rates of -5.17% and -7.11%, respectively. In general, built-up expansion was evident from 2001 to 2018, and cropland, forest, grassland, and water bodies did not change significantly. Nevertheless, forest and water body areas are increasing, and farmland and grassland areas are decreasing (Table

3).

Table 3 Land use and land cover area percentage and change rate for 2001 and 2018

Class	Area 2001	Area 2018	Change Rate
Built-up	0.789%	1.083%	37.26%
Cropland	30.832%	29.237%	-5.17%
Forest	61.917%	63.520%	2.59%
Grassland	5.126%	4.761%	-7.11%
Water bodies	1.336%	1.399%	4.73%

Figure 7 illustrates the spatial distribution of LULCC from 2001 to 2018, wherein significant changes occurred primarily in built-up, cropland, and forest areas. The cropland area experienced a loss caused by both the expansion of major cities and cropland changing into forest land. This is due to the formulation and improvement of North Korea's forest policies, which began in the 1990s [48]. Since 2000, a series of amendments and additions such as the "10-year plan for forest restoration" [51] resulted in the restoration of farmlands into forests [50]. Overall, North Korea has seen significant changes in forest and cropland land cover from 2001 to 2018, although the total area has not changed to a large extent. This lack of total area change is because, although most of the cropland in the southern and central mountainous areas have been converted to forest, the croplands in the western and northern

regions have begun to expand, leading to forest loss.

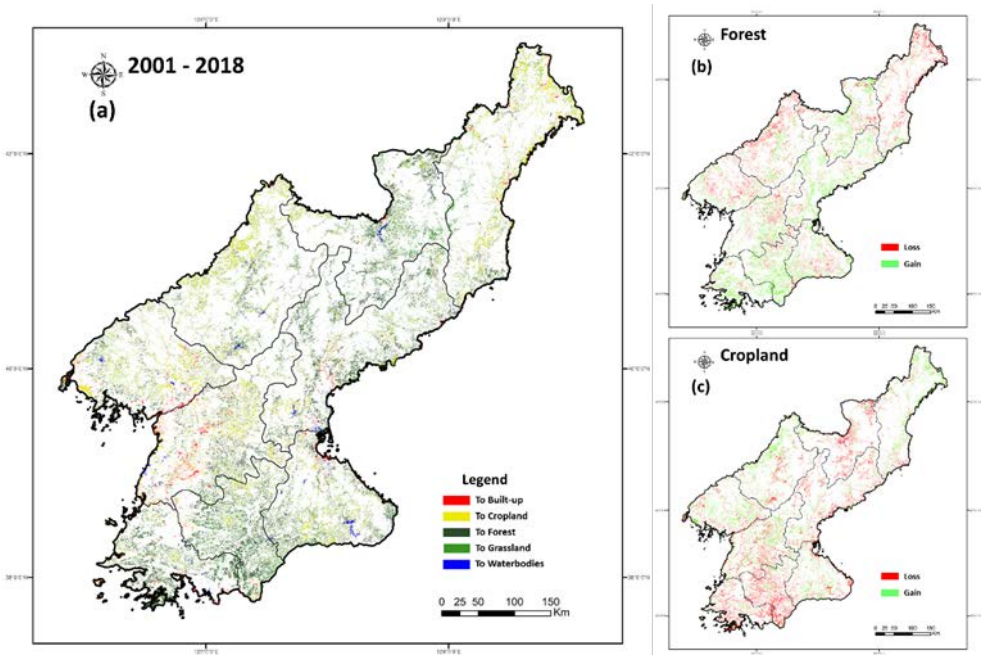

Figure 7 (a) Land use and land cover change map for 2001 and 2018, and (b) Forest land loss and gain, and (c) cropland land loss and gain

4.4. Relation with mountainous cropland and elevation

Figure 8 shows the relationship between forest and cropland areas with elevation from 2001 to 2018. Here, it is clear that below 900 m, the overall area change is uniform, while there is a clear decrease in cropland below 300 m. This decrease occurred because around the time of this study period, new watersheds gradually

began to appear. There-fore, the land that was originally cropland in 2001 was replaced by new watersheds in low-elevation areas in 2018. Above 900 m, there was an increase in forest area and a de-crease in cropland, indicating a decrease in croplands in the mountainous areas of North Korea concomitant with forest restoration. In other words, the mountainous cropland gradually decreased over time as forest restoration continued. In general, at an elevation greater than or equal to 900 m, mountainous croplands were reduced, and forest restoration increased. Meanwhile, the overall change in cropland at less than 900 m was balanced.

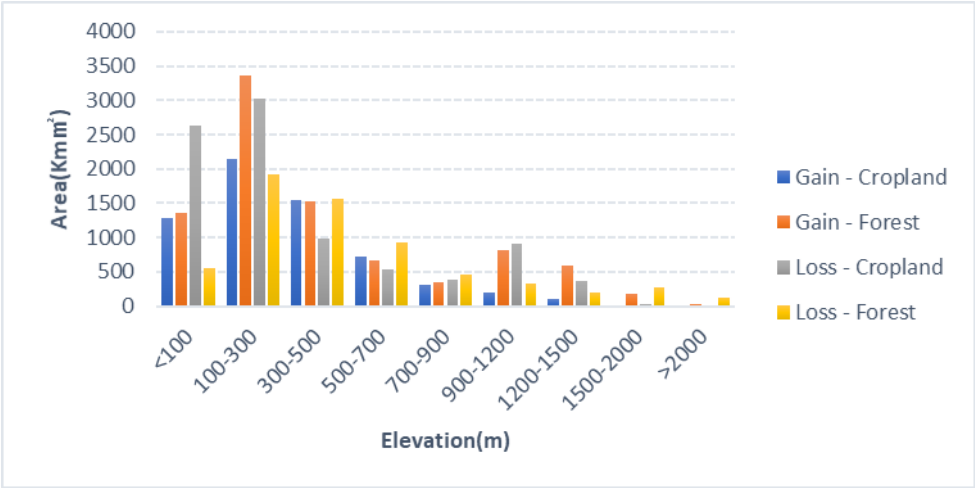

Figure 8 Forest and cropland area loss and gain related to elevation

Chapter 5. Discussion

5.1. Interpretation and explanation of the forest change in North Korea

North Korea is a developing country, with primary industries, including mining, light industry, and agriculture, accounting for its main economic income. According to statistics from 1990 to 2014, agriculture, forestry, and fisheries comprised the second-highest economic income ranking after the service industry. Further, based on estimates from the Bank of Korea, the industrial structure of North Korea, based on the nominal GDP in 2014, comprises 21.8% agriculture, forestry, and fishing; 13.1% mining; 21.3% manufacturing; 31.3% service; and 8.2% construction [52]. This could explain the high contribution of agriculture to North Korea's major economic resources. Since the mid-1970s, North Korea has expanded its mountainous farmlands. On December 11, 1992, North Korea officially enacted the "Forest Law," the first dedicated North Korean forest law [48]. North Korea's continuous expansion of mountainous cropland is somewhat unavoidable, as more than 80% of its land area is mountainous and agriculture is one of its major economic industries. Nevertheless, in June 2000 and October 2001, the Forest Law was strengthened through amendments and

supplements [48]. These amendments were included owing to continued food and energy shortages, as well as the expansion of mountainous cropland and deforestation. The resultant increases in forest areas and human activity have led to a rapidly increasing number of wildfires. In fact, many studies on North Korea have revealed various fundamental problems, including a lack of disaster response capabilities [57], energy shortages [48], a decline in agricultural production [9, 53], and water resource depletion [54, 55], which seems to have had an indirect effect on the strengthening of the Forest Law. Later, on August 2, 2005, in a supplement to a Forest Law amendment, afforestation, reforestation, and restrained logging were emphasized.

Therefore, the development of agriculture, one of North Korea's main economic industries, does not comply with the imposed forest law, which was formulated to reduce deforestation caused by excessive mountainous cropland expansion and deforestation. Therefore, as North Korea enters the modern era, it must conduct reforestation while simultaneously maintaining agriculture as an important economy [56]. Thus, constructing modern geospatial information for North Korea and analyzing its land cover changes is of utmost importance. Through the spatial and geographic analysis of major land cover changes, this study

addresses both the restoration of the southern and central agricultural areas to forest areas and the expansion of western and northern forest areas to agricultural areas.

5.2. Importance of spatial analysis and future research directions

Figures 7 and 8 as well as Table 3 illustrate the differences between the overall numerical LULC change trend and the spatial LULC change trend across North Korea. In the de-tailed spatial analysis, the specific areas and ranges of specific growth or reduction of each LULC type can be determined at the spatial level, and further relevant analyses can be performed according to the characteristics of the change area, such as the driving mechanism [28, 40], or according to the national or regional policy of the change trend [40, 58]. As shown in Figure 8, the change trend can be analyzed on a multi-dimensional level via the spatial analysis, such as via elevation or slope related analysis, to discover more LULCC information [6, 61]. The changes in North Korea's forests and farmland illustrate this aspect. The area changes in North Korea's forests from 2001 to 2018 as shown in Ta-ble 3 are very small, ranging from 61.917% in 2001 to 63.520% in 2018 and increasing only by 1.603%. However, from the spatial change

trends shown in Figure 7, although the overall area of North Korea's forests changes only slightly, the increase in forest cover in southern and central Korea is very clear on a spatial level. The area of farmland in North Korea has also not changed significantly. Table 3 shows a change from 30.832% in 2001 to 29.237% in 2018, implying a decreased by only 1.595%. However, Figure 7 shows that the southern and central regions have decreased significantly in area, and the area of North Korea has increased significantly in the western and northern regions. This shows that in a large-scale LULCC analysis, relying solely on the overall judgment of the data change trend does not yield entirely accurate results. Rather, combining the multi-dimensional space can yield a more accurate judgement of the growth or decrease trend of the LULC. Most of the changes in North Korea's LULC are related to human interference and the impact of national and regional policies [59, 63]. In this regard, more research on spatial change analysis is required in the future. For example, future research can focus on the analysis of the geographical characteristics or related changes in policies according to the division in administrative regions or the location or the watershed [58, 62], and an analysis of the main driving mechanism of the LULC changes according to spatial geographic data, such as the combination of biophysical data

(climate, geology) and human factors (society, economy, politics, culture, and population) [60].

5.3. Limits and Advantages

The semi-permanent point classification method used in this study uses the same pixel values for various data. This may result in land cover classification not being possible in some situations if the land cover class of the study site is diverse and complex or the class area occupied is small. Thus, for North Korea, we incorporated wetland areas in the waterbody land cover type, as wetlands occupy only a small area and cannot be classified. Regarding the overall LULC classification accuracy, as it is difficult to distinguish bare land, grassland, and shrub, which all have similar spectra, the overall accuracy for grassland is much lower than that for the other land cover types [28]. In addition, the timing of satellite image data capture and the amount of data accumulation significantly affect the efficacy of the semi-permanent point classification method. Therefore, data analysis is only available within a limited time series; thus, for LULC classification, only major land cover types can be classified. However, this method is very useful for observing time-series changes, constructing data

for inaccessible areas, and producing highly accurate and reliable results for the major types of land cover. Thus, we can not only obtain high-accuracy time-series LULC maps for inaccessible areas, but also analyze the characteristics of land cover change in the study region.

Chapter 6. Conclusions

An LULC map of North Korea for the period 2001–2018 was constructed using semi-permanent point classification and machine learning techniques based on satellite image time-series data. Using the LULCC detection technique, the overall change in North Korean land cover between 2001 and 2018 and its forest changes were evaluated. Following a classification of land cover of the study area into five categories, built-up, cropland, forest, grassland, and waterbodies (wetland included), our classification accuracy was 97.5% ± 0.9%, and the Kappa coefficient was 0.94 ± 0.02. From 2001 to 2018, the rates of change in the built-up, agricultural, forest, grassland, and waterbody areas were 37.26%, 5.17%, 2.59%, 7.11%, and 4.73%, respectively. In general, with the exception of built-up expansion, land-cover type coverage did not vary considerably. However, distinct spatial changes were observed. The most evident spatial change was the restoration of forests in the southern and central regions and the increase in cropland in the north and west.

By examining the current literature related to North Korea's forests and croplands, we constructed an elevation correlation to make further inferences based on the analysis of land cover change.

Based on this, we propose that one of North Korea's main economic industries is agriculture, which conflicts with the forest protection laws currently in place. To maintain its agricultural industry, North Korea has expanded cropland areas in its mountainous terrain, which comprises 80% of the region. However, with the strengthening of forest protection policies, this mountainous cropland is now the target of reforestation. Furthermore, a correlation analysis between changing cropland and forest areas with elevation revealed that cropland cover is decreasing while forest cover is increasing at elevations above 900 m.

The main purpose of this study was to construct and analyze a modern time-series LULC map and understand forest change trend for North Korea, which is an inaccessible area, using a resolution of 30 m. By examining the characteristics related to cropland and forest cover, we determined that forests in modern North Korea are being restored in certain areas. This indicates that North Korea's forest protection law has begun to have an impact, and cropland cover is being converted to forest cover. Therefore, this result could provide a reference for the study of North Korea's deforestation.

Bibliography

1. McKinley, D. C.; Ryan, M. G.; Birdsey, R. A.; Giardina, C. P.; Harmon, M. E.; Heath, L. S.; Houghton, R. A.; Jackson, R. B.; Morrison, J. F.; Murray, B. C.; Patakl, D. E.; Skog, K. E. A synthesis of current knowledge on forests and carbon storage in the United States. Ecol. Appl. 2011, 21 (6), 1902–1924.
2. Hosonuma, N.; Herold, M.; De Sy, V.; De Fries, R. S.; Brockhaus, M.; Verchot, L.; Angelsen, A.; Romijn, E. An assessment of deforestation and forest degradation drivers in developing countries. Environ. Res. Lett. 2012, 7 (4). 044009.
3. Guadalupe, V.; Sotta, E. D.; Santos, V. F.; Gonçalves Aguiar, L. J.; Vieira, M.; de Oliveira, C. P.; Nascimento Siqueira, J. V. REDD+ implementation in a high forest low deforestation area: constraints on monitoring forest carbon emissions. Land Use Policy 2018, 76, 414–421.
4. Murad, C. A.; Pearse, J. Landsat study of deforestation in the Amazon region of Colombia: departments of Caquetá and Putumayo. Remote Sens. Appl. Soc. Environ. 2018, 11, 161–171.
5. Jeong, S. G.; Park, J.; Park, C. H.; Lee, D. K. Terrace fields classification in north korea using MODIS multi-temporal image data. J. Korea Soc. Environ. Rest. Technol. 2016, 19 (1), 73–83. doi:10.13087/kosert.2016.19.1.73.
6. Choi, W.; Kang, S.; Choi, J.; Larsen, J. J.; Oh, C.; Na, Y.-g. Characteristics of deforestation in the Democratic People's Republic of Korea (North Korea) between the 1980s and 2000s. Reg. Environ. Change 2017, 17 (2), 379–388. doi:10.1007/s10113-016-1022-3.
7. Jin, Y.; Sung, S.; Lee, D. K.; Biging, G. S.; Jeong, S. Mapping deforestation in North Korea using phenology-based multi-index and random forest. Remote Sens. 2016, 8 (12), 997. doi:10.3390/rs8120997.
8. Kang, S.; Choi, W. Forest cover changes in North Korea since the 1980s. Reg. Environ. Change 2014, 14 (1), 347–354. doi:10.1007/s10113-013-0497-4.
9. Lim, C.-H.; Choi, Y.; Kim, M.; Jeon, S. W.; Lee, W.-K. Impact of deforestation on agro-environmental variables in cropland, North Korea. Sustainability 2017, 9 (8), 1354. doi:10.3390/su9081354.
10. Bagan, H.; Millington, A.; Takeuchi, W.; Yamagata, Y. Spatiotemporal analysis of deforestation in the Chapare region

of Bolivia using LANDSAT images. Land Degrad. Dev. 2020, 31 (18), 3024–3039.
11. Margono, B. A.; Turubanova, S.; Zhuravleva, I.; Potapov, P.; Tyukavina, A.; Baccini, A.; Goetz, S.; Hansen, M. C. Mapping and monitoring deforestation and forest degradation in Sumatra (Indonesia) using Landsat time series data sets from 1990 to 2010. Environ. Res. Lett. 2012, 7 (3). 034010.
12. Souza Jr., C. M.; Siqueira, J. V.; Sales, M. H.; Fonseca, A. V.; Ribeiro, J. G.; Numata, I.; Cochrane, M.; Barber, C.; Roberts, D.; Barlow, J. Ten−year Landsat classification of deforestation and forest degradation in the Brazilian Amazon. Remote Sens. 2013, 5 (11), 5493–5513.
13. Gudex−Cross, D.; Pontius, J.; Adams, A. Enhanced forest cover mapping using spectral unmixing and object−based classification of multi−temporal Landsat imagery. Remote Sens. Environ. 2017, 196, 193–204.
14. Gorelick, N.; Hancher, M.; Dixon, M.; Ilyushchenko, S.; Thau, D.; Moore, R. Google Earth Engine: planetary−scale geospatial analysis for everyone. Remote Sens. Environ. 2017, 202, 18–27. doi:10.1016/j.rse.2017.06.031.
15. Viana, C. M.; Girão, I.; Rocha, J. Long−term satellite image time−series for land use/land cover change detection using refined open source data in a rural region. Remote Sens. 2019, 11 (9), 1104.
16. Hütt, C.; Koppe, W.; Miao, Y.; Bareth, G. Best accuracy land use/land cover (LULC) classification to derive crop types using multitemporal, multisensor, and multi−polarization SAR satellite images. Remote Sens. 2016, 8 (8), 684.
17. Ma, J.; Ding, Y.; Cheng, J. C. P.; Jiang, F.; Tan, Y.; Gan, V. J. L.; Wan, Z. Identification of high impact factors of air quality on a national scale using big data and machine learning techniques. J. Cleaner Prod. 2020, 244. 118955.
18. Inglada, J.; Arias, M.; Tardy, B.; Hagolle, O.; Valero, S.; Morin, D.; Dedieu, G.; Sepulcre, G.; Bontemps, S.; Defourny, P.; Koetz, B. Assessment of an operational system for crop type map production using high temporal and spatial resolution satellite optical imagery. Remote Sens. 2015, 7 (9), 12356–12379.
19. Müller, H.; Rufin, P.; Griffiths, P.; Barros Siqueira, A. J. B.; Hostert, P. Mining dense Landsat time series for separating cropland and pasture in a heterogeneous Brazilian savanna landscape. Remote Sens. Environ. 2015, 156, 490–499.
20. Talukdar, S.; Singha, P.; Mahato, S.; Shahfahad; Pal, S.; Liou, Y.; Rahman, A. Land−use land−cover classification by machine

learning classifiers for satellite observations—a review. Remote Sens. 2020, 12 (7), 1135.
21. Kim, S.-W. Land-cover change detection of western DMZ and vicinity using spectral mixture analysis of Landsat imagery. J. Korean Assoc. Geogr. Infor. Stud. 2006, 9 (1), 158-167.
22. Lee, D.-K.; Oh, Y.-C.; Kim, J.-U. A study on forest changes for A/R CDM in North Korea. J. Korea Soc. Environ. Rest. Technol. 2007, 10, 97-104.
23. Piao, D.; Lee, W.-K.; Zhu, Y.; Kim, M.; Song, C. Assessment of forest degradation and carbon storage for REDD+ project in North Korea. Korean J. Environ. Biol. 2016, 34 (1), 1-7.
24. Kang, B.-S. Hydrometeorological climate change trend. Meteor. Technol. Pol. Meteor. Admin. 2009, 2(2), 61-63. (in Korean)
25. Farr, T. G.; Rosen, P. A.; Caro, E.; Crippen, R.; Duren, R.; Hensley, S.; Kobrick, M.; Paller, M.; Rodriguez, E.; Roth, L.; Seal, D.; Shaffer, S.; Shimada, J.; Umland, J.; Werner, M.; Oskin, M.; Burbank, D.; Alsdorf, D. The shuttle radar topography mission. Rev. Geophys. 2007, 45 (2). doi:10.1029/2005RG000183.
26. Elvidge, C. D.; Baugh, K. E.; Kihn, E. A.; Kroehl, H. W.; Davis, E. R. Mapping city lights with nighttime data from the DMSP operational linescan system. Photogramm. Eng. Remote Sens. 1997, 63 (6), 727-734. Retrieved from <Go to ISI>://WOS:A1997XC40700009.
27. Miller, S. D.; Straka, W.; Mills, S. P.; Elvidge, C. D.; Lee, T. F.; Solbrig, J.; Walther, A.; Heidinger, A.; Weiss, S. C. Illuminating the capabilities of the Suomi national polar-orbiting partnership (NPP) visible infrared imaging radiometer suite (VIIRS) Day/Night Band. Remote Sens. 2013, 5 (12), 6717-6766. doi:10.3390/rs5126717.
28. Hu, Y.; Hu, Y. Land cover changes and their driving mechanisms in Central Asia from 2001 to 2017 supported by Google Earth Engine. Remote Sens. 2019, 11 (5). doi:10.3390/rs11050554.
29. Hansen, M. C.; Potapov, P. V.; Moore, R.; Hancher, M.; Turubanova, S. A.; Tyukavina, A.; Thau, D.; Stehman, S. V.; Goetz, S. J.; Loveland, T. R.; Kommareddy, A.; Egorov, A.; Chini, L.; Justice, C. O.; Townshend, J. R. High-resolution global maps of 21st-century forest cover change. Science 2013, 342 (6160), 850-853. doi:10.1126/science.1244693.
30. Chen, J.; Chen, J.; Liao, A.; Cao, X.; Chen, L.; Chen, X.; He, C.; Han, G.; Peng, S.; Lu, M.; Zhang, W.; Tong, X.; Mills, J. Global land cover mapping at 30 m resolution: a POK-based operational approach. I.S.P.R.S. J. Photogramm. 2015, 103, 7-27.

doi:10.1016/j.isprsjprs.2014.09.002.
31. Gong, P.; Wang, J.; Yu, L.; Zhao, Y.; Zhao, Y.; Liang, L.; Niu, Z.; Huang, X.; Fu, H.; Liu, S.; Li, C.; Li, X.; Fu, W.; Liu, C.; Xu, Y.; Wang, X.; Cheng, Q.; Hu, L.; Yao, W.; Zhang, H.; Zhu, P.; Zhao, Z.; Zhang, H.; Zheng, Y.; Ji, L.; Zhang, Y.; Chen, H.; Yan, A.; Guo, J.; Yu, L.; Wang, L.; Liu, X.; Shi, T.; Zhu, M.; Chen, Y.; Yang, G.; Tang, P.; Xu, B.; Giri, C.; Clinton, N.; Zhu, Z.; Chen, J.; Chen, J. Finer resolution observation and monitoring of global land cover: first mapping results with Landsat TM and ETM+ data. Int. J. Remote Sens. 2013, 34 (7), 2607–2654. doi:10.1080/01431161.2012.748992.
32. Li, C.; Gong, P.; Wang, J.; Zhu, Z.; Biging, G. S.; Yuan, C.; Hu, T.; Zhang, H.; Wang, Q.; Li, X.; Liu, X.; Xu, Y.; Guo, J.; Liu, C.; Hackman, K. O.; Zhang, M.; Cheng, Y.; Yu, L.; Yang, J.; Huang, H.; Clinton, N. The first all−season sample set for mapping global land cover with Landsat−8 data. Sci. Bull. 2017, 62 (7), 508–515. doi:10.1016/j.scib.2017.03.011.
33. Oliphant, A.; Thenkabail, P.; Teluguntla, P.; Xiong, J.; Congalton, R.; Yadav, K., . . . Smith, C. NASA making earth system data records for use in research environments (MEaSUREs) global food security−support analysis data (GFSAD) cropland extent 2015. Southeast Asia 30 m V001. http://oar.icrisat.org/id/eprint/10981 2017.
34. Rodriguez−Galiano, V. F.; Ghimire, B.; Rogan, J.; Chica−Olmo, M.; Rigol−Sanchez, J. P. An assessment of the effectiveness of a random forest classifier for land−cover classification. I.S.P.R.S. J. Photogramm. 2012, 67, 93–104.
35. Abdullah, A. Y. M.; Masrur, A.; Adnan, M. S. G.; Baky, M. A. A.; Hassan, Q. K.; Dewan, A. Spatio−temporal patterns of land use/land cover change in the heterogeneous coastal region of Bangladesh between 1990 and 2017. Remote Sens. 2019, 11 (7), 790. doi:10.3390/rs11070790.
36. DeFries, R. S.; Townshend, J. R. G. NDVI−derived land cover classifications at a global scale. Int. J. Remote Sens. 1994, 15 (17), 3567–3586. doi:10.1080/01431169408954345.
37. Gao, B.−C. NDWI−A normalized difference water index for remote sensing of vegetation liquid water from space. Remote Sens. Environ. 1996, 58 (3), 257–266. doi:10.1016/S0034−4257(96)00067−3.
38. Xiong, J.; Thenkabail, P. S.; Tilton, J. C.; Gumma, M. K.; Teluguntla, P.; Oliphant, A.; Congalton, R.; Yadav, K.; Gorelick, N. Nominal 30−m cropland extent map of continental Africa by integrating pixel−based and object−based algorithms using

Sentinel-2 and Landsat-8 data on Google Earth Engine. Remote Sens. 2017, 9 (10), 1065. doi:10.3390/rs9101065.
39. Lu, D.; Li, G.; Moran, E.; Hetrick, S. Spatiotemporal analysis of land-use and land-cover change in the Brazilian Amazon. Int. J. Remote Sens. 2013, 34 (16), 5953-5978. doi:10.1080/01431161.2013.802825.
40. Tian, Y.; Yin, K.; Lu, D.; Hua, L.; Zhao, Q.; Wen, M. Examining land use and land cover spatiotemporal change and driving forces in Beijing from 1978 to 2010. Remote Sens. 2014, 6 (11), 10593-10611.
41. Ghosh, A.; Sharma, R.; Joshi, P. K. Random forest classification of urban landscape using Landsat archive and ancillary data: combining seasonal maps with decision level fusion. Appl. Geogr. 2014, 48, 31-41.
42. Liu, D.; Chen, N.; Zhang, X.; Wang, C.; Du, W. Annual large-scale urban land mapping based on Landsat time series in Google Earth Engine and OpenStreetMap data: a case study in the Middle Yangtze river basin. I.S.P.R.S. J. Photogramm. 2020, 159, 337-351.
43. Yu, J.-S.; Park, C.-H.; Lee, S.-H. Level 3 type land use land cover (LULC) characteristics based on phenological phases of North Korea. Korean J. Remote Sens. 2011, 27 (4), 457-466. doi:10.7780/kjrs.2011.27.4.457.
44. Hong, S.-Y.; Rim, S.-K.; Lee, S.-H.; Lee, J.-C.; Kim, Y.-H. Spatial anaylsis of agro-environment of North Korea using remote sensing I. Landcover classification from Landsat TM imagery and topography analysis in North Korea. Korean J. Environ. Agric. 2008, 27 (2), 120-132. doi:10.5338/KJEA.2008.27.2.120.
45. Bock, G.-W.; Zmud, R. W.; Kim, Y.-G.; Lee, J.-N. Behavioral intention formation in knowledge sharing: examining the roles of extrinsic motivators, social-psychological forces, and organizational climate. M.I.S. Q. 2005, 29 (1), 87-111.
46. Fielding, A. H.; Bell, J. F. A review of methods for the assessment of prediction errors in conservation presence/absence models. Environ. Conserv. 1997, 24 (1), 38-49.
47. Yu, J.; Kim, K. Spatiotemporal changes and drivers of deforestation and forest degradation in North Korea. J. Korean Soc. Environ. Rest. Technol. 2015, 73-83.
48. Park, K.; Lee, S.; Park, S. A study on the North Korea's change of forest policy since the economic crisis in 1990s. Korean J. Unification Aff. 2009, 21, 459-492.

49. National Institute of Forest Science. Development of a method of constructing North Korean forest information using satellite imagery and AI; National Institute of Forest Science. (in Korean), 2020.
50. Yu, J.; Park, H.; Lee, S.-h.; Kim, K. Review of slope criteria and forestland restoration plan in North Korea. J. Korean 2016 Yu, J.; Park, H.; Lee, S.; Kim, K.. J. Korea Soc. Environ. Rest. Technol. 2016, 19 (4), 19-28. doi:10.13087/kosert.2016.19.4.19.
51. Oh, S.; Kim, E.; Kim, K. Characteristics of forest policy in the Kim Jong-Un era. North Korean Stud. 2018, 14 (2), 101-133.
52. Lee, S. North Korean Industrial Statistics; Industrial Research Institute (in Korean), 2015.
53. Ryu, J.-H.; Han, K.-S.; Lee, Y.-W.; Park, N.-W.; Hong, S.; Chung, C.-Y.; Cho, J. Different agricultural responses to extreme drought events in neighboring counties of South and North Korea. Remote Sens. 2019, 11 (15), 1773. doi:10.3390/rs11151773.
54. Kim, K.-h.; Choi, K.-w.; Kim, I.-s.; Noh, S.-i. North Korea's Agricultural Irrigation System; Vol. 2014; Korean Society of Agricultural Engineers, 2014, pp 129-129.
55. Kim, K.-h.; Jin, W.-g. Water Resources of North Korea; Vol. 2013; Korean Society of Agricultural Engineers, 2013, pp 102-102.
56. Lee, S. North Korea's Industry Trends in 2017. [KDI] North Korean Economy [Review, 20] 2018, 2. (in Korean).
57. Lee, B.-R.; Oh, S.-B.; Byun, H.-R. The characteristics of drought occurrence in North Korea and its comparison with drought in South Korea. Theoretical and Applied Climatology 2014, 121, 199-209, doi:10.1007/s00704-014-1230-z.
58. Daunt, A.B.P.; Silva, T.S.F. Beyond the park and city dichotomy: Land use and land cover change in the northern coast of São Paulo (Brazil). Landscape and Urban Planning 2019, 189, 352-361, doi:10.1016/j.landurbplan.2019.05.003.
59. Kim, E.-S.; Lee, S.-H.; Cho, H.-K. Segment-based land cover classification using texture Information in degraded forest land of north korea. Korean Journal of Remote Sensing 2010, 26, 477-487.
60. Kleemann, J.; Baysal, G.; Bulley, H.N.; Fürst, C. Assessing driving forces of land use and land cover change by a mixed-method approach in north-eastern Ghana, West Africa. Journal of Environmental Management 2017, 196, 411-442, doi:10.1016/j.jenvman.2017.01.053.

61. Lone, S.A.; Mayer, I.A. Geo-spatial analysis of land use/land cover change and its impact on the food security in District Anantnag of Kashmir Valley. GeoJournal 2019, 84, 785-794.
62. Muriithi, F.K. Land use and land cover (LULC) changes in semi-arid sub-watersheds of Laikipia and Athi River basins, Kenya, as influenced by expanding intensive commercial horticulture. Remote Sensing Applications: Society and Environment 2016, 3, 73-88.
63. Song, X.-P.; Hansen, M.C.; Stehman, S.V.; Potapov, P.V.; Tyukavina, A.; Vermote, E.F.; Townshend, J.R. Global land change from 1982 to 2016. Nature 2018, 560, 639-643, doi:10.1038/s41586-018-0411-9.
64. Turner, B.L.; Lambin, E.F.; Reenberg, A. The emergence of land change science for global environmental change and sustainability. Proceedings of the National Academy of Sciences 2007, 104, 20666-20671, doi:10.1073/pnas.0704119104.
65. Obodai, J.; Adjei, K.A.; Odai, S.N.; Lumor, M. Land use/land cover dynamics using landsat data in a gold mining basin-the Ankobra, Ghana. Remote Sensing Applications: Society and Environment 2019, 13, 247-256, doi:10.1016/j.rsase.2018.10.007.
66. Teixeira, Z.; Teixeira, H.; Marques, J.C. Systematic processes of land use/land cover change to identify relevant driving forces: Implications on water quality. Science of the Total Environment 2014, 470, 1320-1335, doi:10.1016/j.scitotenv.2013.10.098.
67. Zhao, S.; Peng, C.; Jiang, H.; Tian, D.; Lei, X.; Zhou, X. Land use change in Asia and the ecological consequences. Ecological Research 2006, 21, 890-896, doi:10.1007/s11284-006-0048-2.
68. Foody, G.M.; Mathur, A. Toward intelligent training of supervised image classifications: directing training data acquisition for SVM classification. Remote Sensing of Environment 2004, 93, 107-117.
69. Prasad, A.M.; Iverson, L.R.; Liaw, A. Newer classification and regression tree techniques: bagging and random forests for ecological prediction. Ecosystems 2006, 9, 181-199.
70. Richards, J.A.; Richards, J. Remote sensing digital image analysis; Springer: 1999; Volume 3.
71. Breiman, L. Random forests. Machine learning 2001, 45, 5-32, doi:10.1023/A:1010933404324.
72. Naghibi, S.A.; Pourghasemi, H.R.; Dixon, B. GIS-based groundwater potential mapping using boosted regression tree,

classification and regression tree, and random forest machine learning models in Iran. Environmental monitoring and assessment 2016, 188, 1-27.
73. Shabani, S.; Jaafari, A.; Bettinger, P. Spatial modeling of forest stand susceptibility to logging operations. Environmental Impact Assessment Review 2021, 89, 106601.
74. Manandhar, R.; Odeh, I.O.; Ancev, T. Improving the accuracy of land use and land cover classification of Landsat data using post-classification enhancement. Remote Sensing 2009, 1, 330-344.
75. Smits, P.; Dellepiane, S.; Schowengerdt, R. Quality assessment of image classification algorithms for land-cover mapping: a review and a proposal for a cost-based approach. International journal of remote sensing 1999, 20, 1461-1486.
76. Congalton, R.G. A review of assessing the accuracy of classifications of remotely sensed data. Remote sensing of environment 1991, 37, 35-46.
77. Foody, G.M. Status of land cover classification accuracy assessment. Remote sensing of environment 2002, 80, 185-201.
78. Liu, C.; Frazier, P.; Kumar, L. Comparative assessment of the measures of thematic classification accuracy. Remote sensing of environment 2007, 107, 606-616.

Appendix

Table A 1 Reclassification between different LULC projects used in this study

Class	FROMGLC2017	GLC30	GFCD	GFSAD30SEACE	MCD12Q1.006
Urban	8	80	-	-	13
Cropland	1	10	-	2	12 14
Forest	2	20	treecover2000	-	1 2 3 4 5
Grassland	3 4	30 40	-	-	6 7 8 9 10
Bareland	7 9	90	-	-	16
Water bodies add Wetland	5 6	50 60	-	0	11 17

Finer Resolution Observation and Monitoring of Global Land Cover (FROM-GLC) code: 1 Cropland, 2 Forest, 3 Grassland, 4 Shrubland, 5 Wetland, 6 Water, 7 Tundra, 8 Impervious surface, 9 Bareland, 10 Snow/Ice

Global land cover (GLC30) code: 10 Cultivated land, 20 Forest, 30 Grassland, 40 Shrubland, 50 Wetland, 60 Water bodies, 80 Artificial surfaces, 90 Bareland

Global Forest Change dataset (GFCD) code: treecover2000

Global Food Security-support Analysis Data Extent Southeast and Northeast Asia (GFSAD30SEACE) code: 0 Water, 1 Non-Cropland, 2 Cropland

MCD12Q1.006 code: 1 Evergreen Needleleaf Forests: dominated by

evergreen conifer trees (canopy >2m). Tree cover >60%, 2 Evergreen Broadleaf Forests: dominated by evergreen broadleaf and palmate trees (canopy >2m). Tree cover >60%, 3 Deciduous Needleleaf Forests: dominated by deciduous needleleaf (larch) trees (canopy >2m). Tree cover >60%, 4 Deciduous Broadleaf Forests: dominated by deciduous broadleaf trees (canopy >2m). Tree cover >60%, 5 Mixed Forests: dominated by neither deciduous nor evergreen (40-60% of each) tree type (canopy >2m). Tree cover >60%, 6 Closed Shrublands: dominated by woody perennials (1-2m height) >60% cover, 7 Open Shrublands: dominated by woody perennials (1-2m height) 10-60% cover, 8 Woody Savannas: tree cover 30-60% (canopy >2m), 9 Savannas: tree cover 10-30% (canopy >2m), 10 Grasslands: dominated by herbaceous annuals (<2m), 11 Permanent Wetlands: permanently inundated lands with 30-60% water cover and >10% vegetated cover, 12 Croplands: at least 60% of area is cultivated cropland, 13 Urban and Built-up Lands: at least 30% impervious surface area including building materials, asphalt and vehicles, 14 Cropland/Natural Vegetation Mosaics: mosaics of small-scale cultivation 40-60% with natural tree, shrub, or herbaceous vegetation, 15 Permanent Snow and Ice: at least 60% of area is covered by snow and ice for at least 10 months of the year, 16 Barren: at least 60% of area is non-vegetated barren (sand, rock, soil) areas with less than 10% vegetation, 17 Water Bodies: at least 60% of area is covered by permanent water bodies.

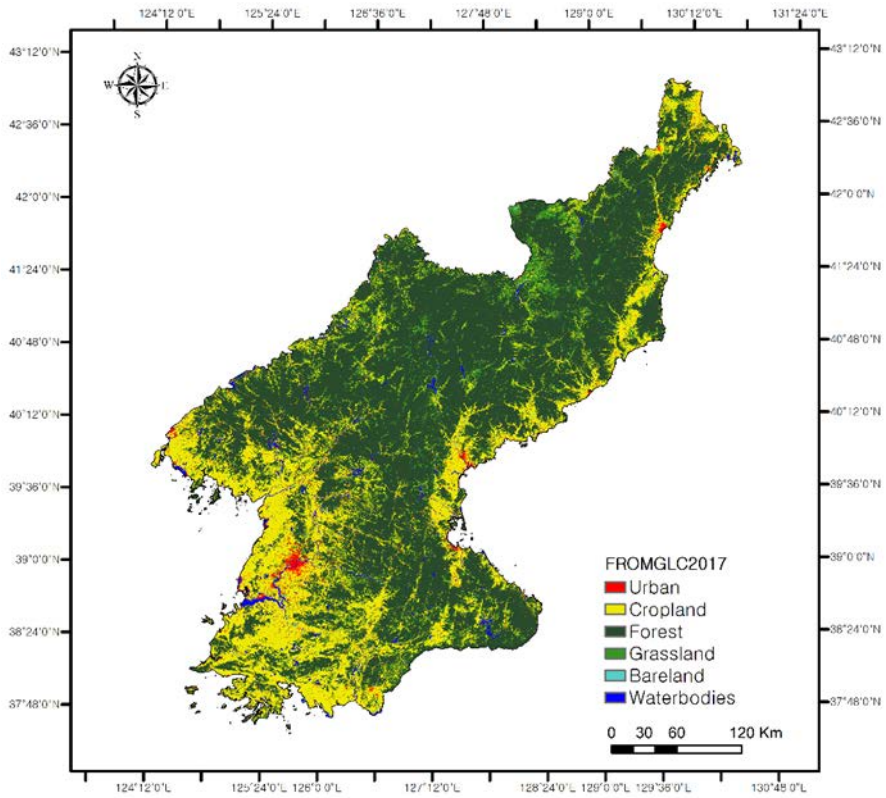

Figure A 1 Reclassification of Land Use Land Cover Products: Finer Resolution Observation and Monitoring of Global Land Cover (FROM-GLC)

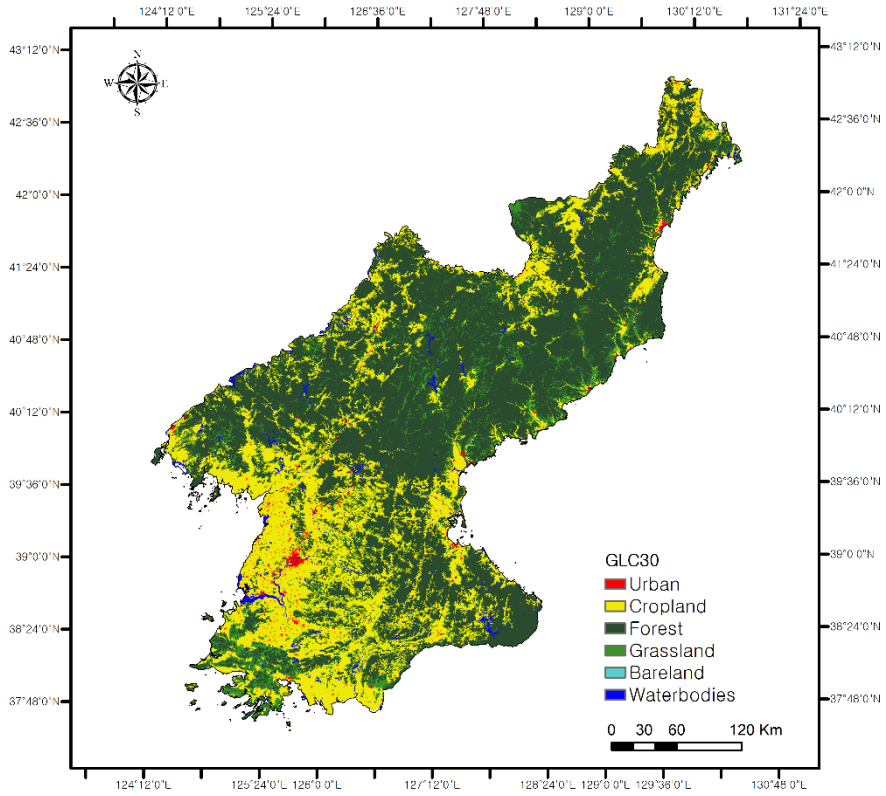

Figure A 2 Reclassification of Land Use Land Cover Products: Global land cover (GLC30)

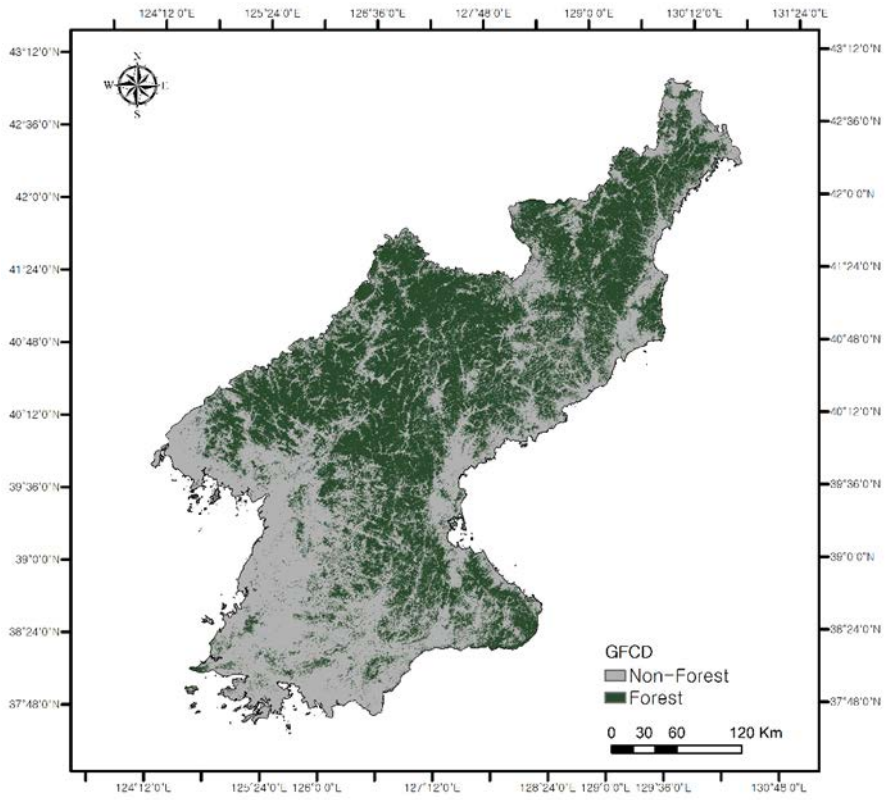

Figure A 3 Reclassification of Land Use Land Cover Products: Global Forest Change dataset (GFCD)

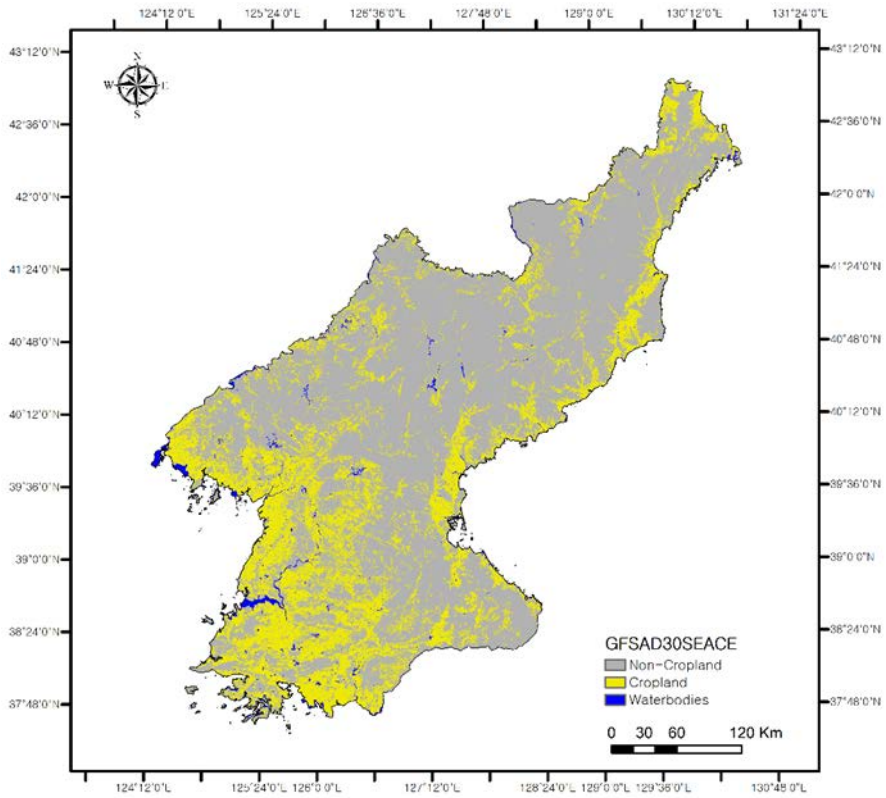

Figure A 4 Reclassification of Land Use Land Cover Products: Global Food Security-support Analysis Data Extent Southeast and Northeast Asia (GFSAD30SEACE)

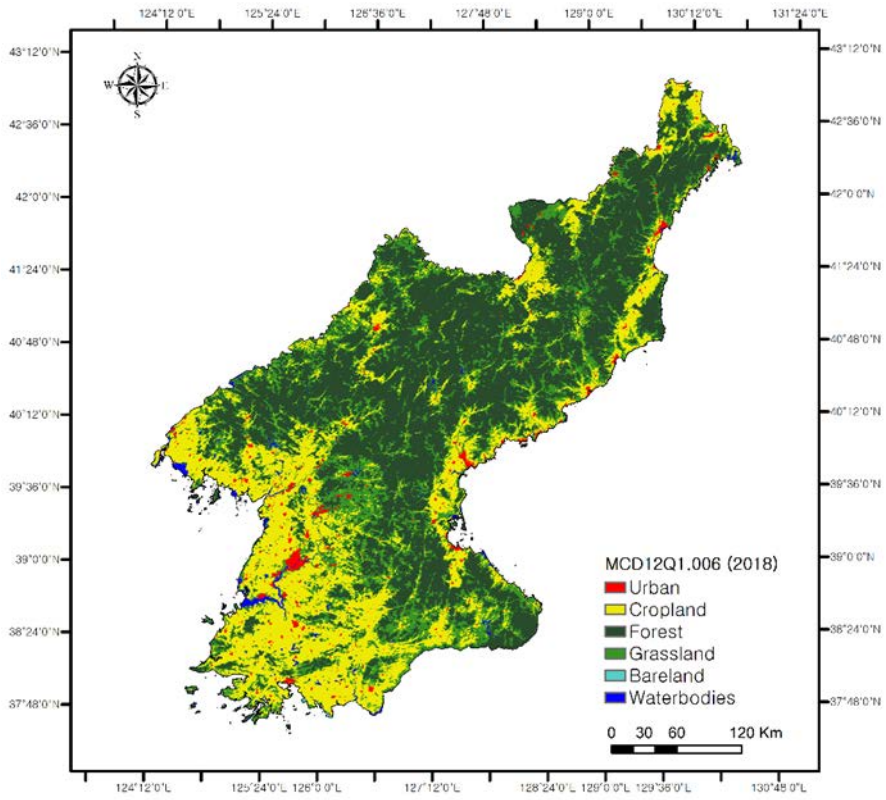

Figure A 5 Reclassification of Land Use Land Cover Products: MCD12Q1.006

Abstract in Korean

북한은 세계에서 가장 심각하게 황폐화된 산림 중 하나를 포함하고 있지만 최근에는 산림 복원을 강조하고 있다. 산림 복원이 일어나는 정도를 이해하기 위해서는 토지 이용과 토지 피복 변화 경향(LULCC)을 이해해야 한다. 따라서 본 연구는 30m 해상도의 현대 시계열 토지 이용 토지 피복 (LULC)지도를 구성 및 분석하여 북한 전역의 장기 LULCC를 식별하고 산림 변화 추세를 이해하는 것을 목표로 한다. 2001 – 2018 년 기간 동안 국가의 LULC지도는 30m 해상도 위성 이미지 시계열 데이터를 기반으로 반영구적 포인트 분류 및 기계 학습을 사용하여 구성되었으며, 이는 GEE (Google Earth Engine)에서 수집 한 현상 학적 정보와 함께 사용되고 있다. 또한 LULCC 탐지기 법과 경작지 변화와 고도의 관계를 고려하여 2001 – 2018 년 북한의 산림 변화를 평가하였다. LULC 맵 결과의 전체 분류 정확도는 97.5 % ± 0.9 %이고, Kappa 계수는 0.94 ± 0.02 이다. LULCC 탐지는 또한 2001 – 2018 년에 북한의 산림 면적이 약간 증가한 것으로 나타났다. 일반적으로 산림 피복 면적은 크게 변하지 않았으나 남부와 중부 지역의 산림 복원과 북부와 서부의 경작지 상대적 증가 측면에서 뚜렷한 공간적 변화가 관찰되었다. 북한의 특성과 산림 정책 문서를 검토 한 결과 북한 근대 산림의 일부 지역이 복원되고 있음을 확인하였다.

Keyword : 토지이용 및 토지피복 변화, NDWI, NDVI, 산림, 농업, 북한

Student Number : 2019-21805